Numerical calculation of a dressed photon energy transfer based on a quantum walk model

M. Ohtsu[1], E. Segawa[2], and K. Yuki[3]

[1]Research Origin for Dressed Photon,3-13-19 Moriya-cho, Kanagawa-ku, Yokohama, Kanagawa 221-0022, Japan

[2]Yokohama National University, 79-8 Tokiwadai, Hodogaya-ku, Yokohama, Kanagawa 240-8501, Japan

[3]Middenii, 3-3-13 Nishi-shinjuku, Sinjuku-ku, Tokyo 160-0023, Japan

Abstract

To study the probability of a dressed-photon–phonon (DPP) created on the tip of a fiber probe based on a quantum walk (QW) model, the creation probability of the DPP at the apex of a two-dimensional triangular lattice is numerically calculated by substituting several values of mathematical (ξ) and physical (χ / J) parameters. Two cases are dealt with: One is the case in which the DPP energy does not dissipate from the slope of the triangular lattice; and the other is the case in which the DPP energy dissipates. It is found that the optimum value of ξ is 67.5 degree, and the value of χ / J can be fixed to 1. The calculated temporal behaviors agree with the results derived by QW theory.

1. Introduction

A dressed photon (DP) is a quantum field that is created as the result of an interaction between photons and excitons (pairs consisting of electrons and positive holes) in a nanometer-sized particle (NP). It localizes on the NP and its size is much smaller than the wavelength of light. It is an off-shell field because its momentum has a large uncertainty originating from its sub-wavelength size [1,2]. Conventional on-shell scientific theories cannot be used to analyze this field because no thorough studies of this light–matter interaction have been made in the long history of on-shell science. Fortunately, however, studies of this interaction in off-shell science have commenced recently, resulting in a precise description of the mechanism of DP creation [3,4].

After the DP is created on a NP, it hops to adjacent NPs. During this hopping, the DP excites a crystal lattice vibration, resulting in the creation of a phonon. The created phonon interacts with the DP to form a new state of the DP, which is called a dressed-photon–phonon (DPP) [5]. The DPP energy transfers through adjacent NPs. Although the tempo-spatial behavior of this transfer has been experimentally evaluated, it has not been fully described by conventional theories of a random walk process [6]. In order to describe the behavior, a quantum walk (QW) model was recently employed, allowing the unique properties of the DPP to be analyzed [7].

In this article, the probability of DPP creation on the tip of a fiber probe is numerically calculated based on the QW model, and the results are compared with experimental results.

2. Purpose and method

The present calculations are based on a two-dimensional QW model for simplicity. Figure 1(a) shows a right-angled isosceles triangular lattice that approximates the profile of the fiber probe. Figure 1(b) schematically explains that, by applying input signals to all the sites on the base of the triangular lattice, DPs are created and transferred to the adjacent sites. During this transfer, DPPs are created by the DP–phonon interaction. These DPPs transfer through the triangular lattice and finally reach its apex (the tip of the fiber probe). This apex is assumed to be a sink from which the DPP energy is dissipated. This article calculates the creation probability P of the DPP at this sink.

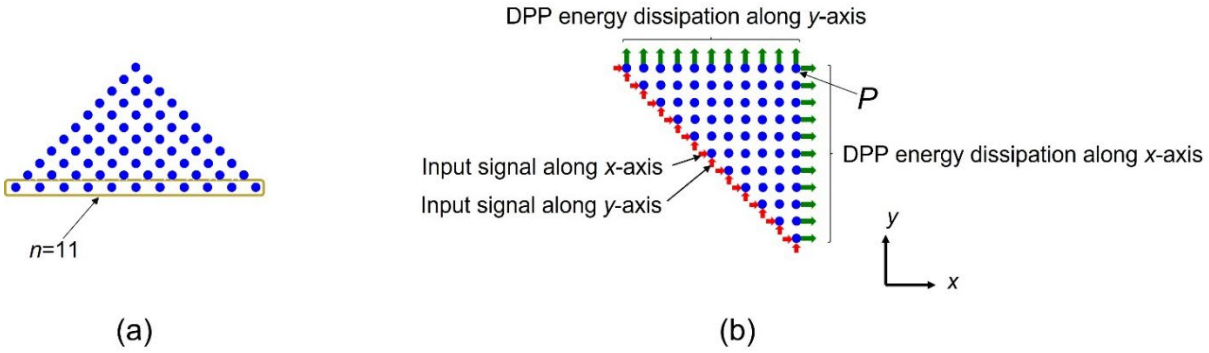

Fig. 1 A two-dimensional right-angled isosceles triangular lattice.
(a) The case of n =11. (b) The lattice illustrated after rotating that in (a) by 45 degree for convenience of the numerical calculation.

Three parameters are used for the calculation:

(1) Mathematical parameter ξ:

To cover a broader range of mathematical discussions based on the QW model, a phase angle ξ is introduced to the real-valued matrix in eq. (6) of ref. [7]:

$$U = \begin{bmatrix} \varepsilon_+ & J & \chi \\ J & \varepsilon_- & \chi \\ \chi & \chi & \varepsilon_0 \end{bmatrix}. \qquad (1)$$

As a result, U is replaced by a complex-valued matrix

$$U(\xi) = \exp(i\xi)U\,. \qquad (2)$$

Here, ξ is regarded as a mathematical parameter.

(2) Physical parameter χ / J:

Since the quantities J and χ in eq. (1) represent the energies of the DP-hopping to the adjacent NP (an atom in the fiber probe) and of the DP–phonon interaction, respectively, their ratio χ / J is regarded as a physical parameter. The value of χ / J may be fixed to 1 for simplicity, as was

recommended in ref. [7]. However, to cover a broader range of physical discussions, the present article employs a wider range of values, i.e., $0.1 \le \chi / J \le 10$.

(3) Parameter n for numerical calculation:

The total number of sites increases as the number n of sites on the base of the triangular lattice increases. Since this increase can improve the accuracy of approximating the fiber probe by the triangular lattice, n is regarded as a parameter for the numerical calculation.

The probability P is numerically calculated by substituting several values of ξ and χ / J into eqs. (1) and (2).

Section 3 deals with two cases: One is the case in which the DPP energy does not dissipate from the slope of the triangular lattice. The other is the case in which the DPP energy dissipates. For the former case, the tempo-spatial evolution equation at the slope is given by eq. (12a) in ref. [7], which is

$$\vec{\psi}^{\Leftrightarrow}_{t+1,(x,y)} = \sigma P_{-}^{\Updownarrow} \vec{\psi}^{\Updownarrow}_{t,(x,y)} + P_{-}^{\Updownarrow} \vec{\psi}^{\Updownarrow}_{t,(x+1,y)} + P_{0}^{\Updownarrow} \vec{\psi}^{\Updownarrow}_{t,(x,y)} . \tag{3}$$

Here, the matrix σ represents the DPP energy reflection at the slope. For the latter, the equation, given by eq. (10b) in ref. [7], is

$$\vec{\psi}^{\Updownarrow}_{t+1,(x,y)} = P_{+}^{\Leftrightarrow} \vec{\psi}^{\Leftrightarrow}_{t,(x,y-1)} + P_{-}^{\Leftrightarrow} \vec{\psi}^{\Leftrightarrow}_{t,(x,y+1)} + P_{0}^{\Leftrightarrow} \vec{\psi}^{\Leftrightarrow}_{t,(x,y)} . \tag{4}$$

3. Results and discussion

After the input signals are applied to all the sites on the base of the triangular lattice simultaneously, the value of P increases with time and reaches a stationary value. Subsection 3.1 discusses the dependence of the stationary value of P on the parameters in eqs. (1) to (3) in Section 2. Subsection 3.2 presents temporal behaviors of P prior to converging to the stationary value.

3.1 Dependences of the probability on mathematical and physical parameters

Figure 2 shows the external forms and cross-sectional structures of fiber probes [8]. The DPP energy dissipates from the taper of the fiber probe. This corresponds to radiating scattered light from the taper. In order to avoid this radiation, an opaque metallic film is formed on the taper (Fig. 2(a)) to realize a high-efficiency fiber probe. This is the prototype of devices that are now popularly used. Figure 2(b) is a basic fiber probe without a metallic film coating, resulting in DPP energy dissipation from the taper. This is a primitive device that was used only in the early stages of DP science. Figures 2(c) and (d) are for advanced devices, i.e., asymmetric and triple-tapered fiber probes, respectively, for future numerical calculations (cf. Section 4). Corresponding to Figs. 2(a) and (b), numerical calculations are carried out for the two cases presented in Section 2.

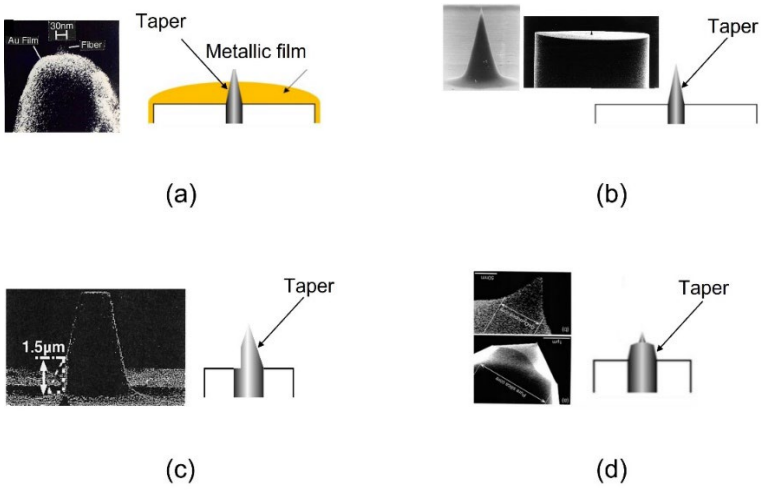

Fig. 2 External forms and cross-sectional structures of the fiber probes.
(a) A high-efficiency fiber probe with an opaque metallic film on the taper. (b) A basic fiber probe. (c) An asymmetric fiber probe. (d) A triple-tapered fiber probe.

Case 1: Without DPP energy dissipation

Figure 3 shows the calculated results of the dependence of the probability P on the parameters ξ and χ / J. The parameter n was fixed to 5, 11, 21, and 41 in Figs. 3(a)-(d). The values of P at χ / J =1 are extracted from these figures, and their dependences on ξ are shown in Figs. 4(a) – (d). The curves in these figures show a lot of bumps that are attributed to interference in the triangular lattice originating from reflection at the slope. The interval between the adjacent bumps (indicated by horizontal double arrows) decreases as n increases, as is shown by Fig. 5. These decreases indicate that the magnitude of the interference decreases with an increase in the size of the triangular lattice. Since this interference had not been experimentally observed, the present calculation results are quite reasonable.

Figure 4 shows that the value of P takes the maximum $P_{\max}$ at ξ =67.5 degree. This value of ξ is equal to (3/8)π. The reason why the rational number 3/8 appears here should be studied in the future. Figure 6 shows the dependence of this maximum $P_{\max}$ on n. It is found from this figure that the maximum $P_{\max}$ increases roughly monotonically with the increase of n. This means that the DPP energy is effectively confined in the triangular lattice due to reflection at the slope, which agrees with the characteristics of the actual high-efficiency fiber probe in Fig. 2(a). However, the values deviate from this monotonic increase in the range $n < 21$, which may be due to interference inside the triangle.

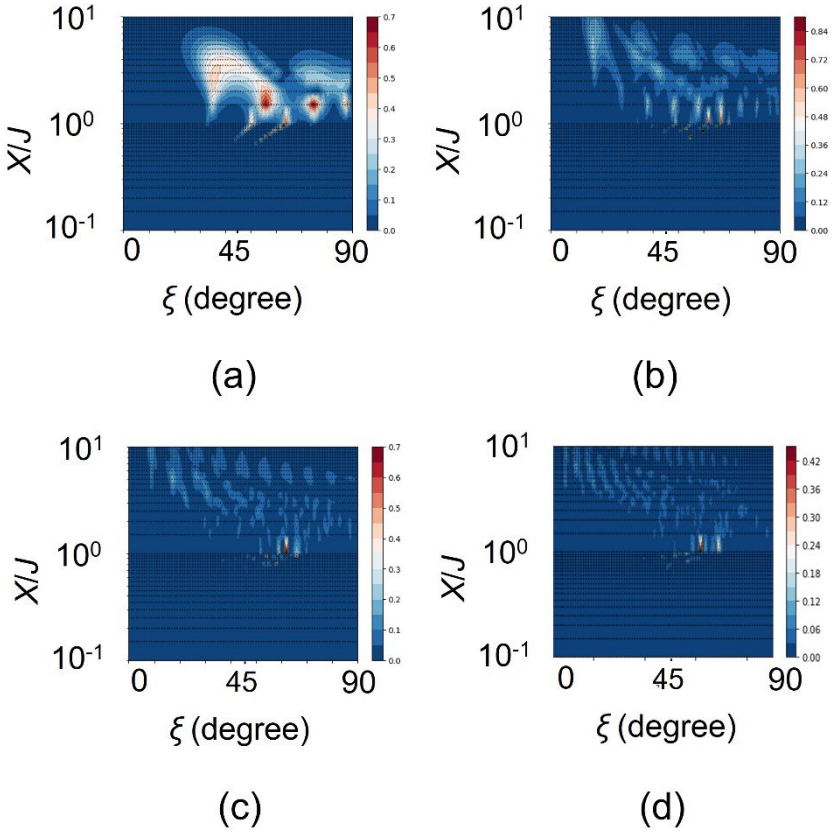

Fig.3 Dependence of P on ξ and χ / J in the case without DPP energy dissipation. n is 5 (a), 11 (b), 21 (c), and 41 (d).

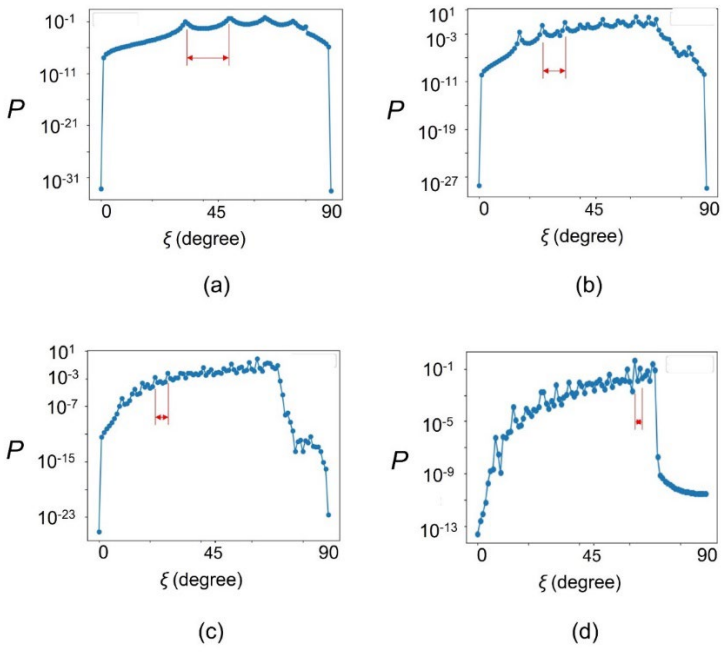

Fig.4 Dependence of P on ξ at χ / J =1. n is 5 (a), 1 1(b), 21 (c), and 41 (d). Horizontal double arrows indicate the interval of the adjacent bumps.

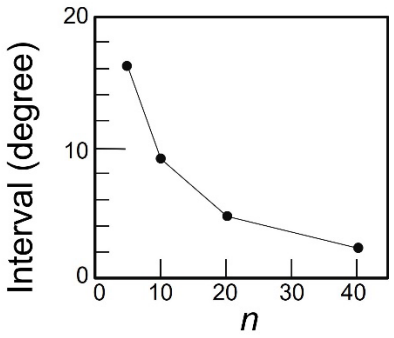

Fig. 5 Dependence of the interval between the adjacent bumps on n.

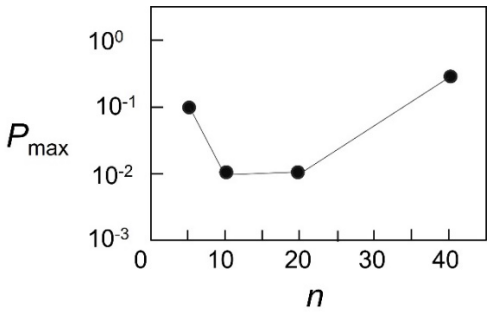

Fig. 6 Dependence of the maximum $P_{\max}$ (in Fig. 4) on n.

Figure 7 shows the ratio between the maximum $P_{\max}$ and minimum $P_{\min}$ of the curves in Figs. 4(a) – (d). The ratio monotonically decreases with the increases of n. This decrease also indicates that the effects of reflection and interference become less conspicuous, which means that the present calculation results agree with the experimental results.

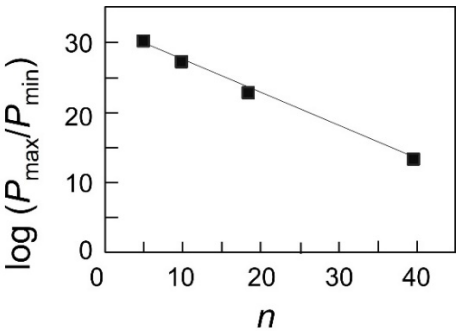

Fig. 7 Dependence of the ratio between the maximum $P_{\max}$ and minimum $P_{\min}$ (in Fig. 4) on n.

Case 2: With DPP energy dissipation

Figure 8 shows the calculated results of the dependence of P on ξ and χ / J. In Figs. 8(a)-(d), n is fixed to 5, 11, 21, and 41. Crescent-shaped red belts are seen in the upper right parts of these figures, in which the value of P is very large in comparison with those outside the red belts. It takes the maximum value at the position □ at ξ=90 degree. The origin of these red belts is attributed to

intrinsic properties of the QW or dispersive features of the phonon energy. The values of P show irregular variations and abrupt increases in the red belts and at their rims. The value of χ/J at □ increases with the increases of n, as is shown by Fig. 9. It increases to $\chi/J \gg 1$, which means that the value of P at $\chi/J=1$ (as was recommended in ref.[7]) does not vary irregularly with ξ. For reference, the value of P at χ/J=5 takes the maximum at the position ○ in Fig. 8. The value of ξ at this position ○ irregularly varies with the increase of n, as is shown by Fig. 10. A possible reason for this irregularity is that the red belt passes through the horizontal line χ/J=5 in Fig. 8 when n varies from 11 to 41.

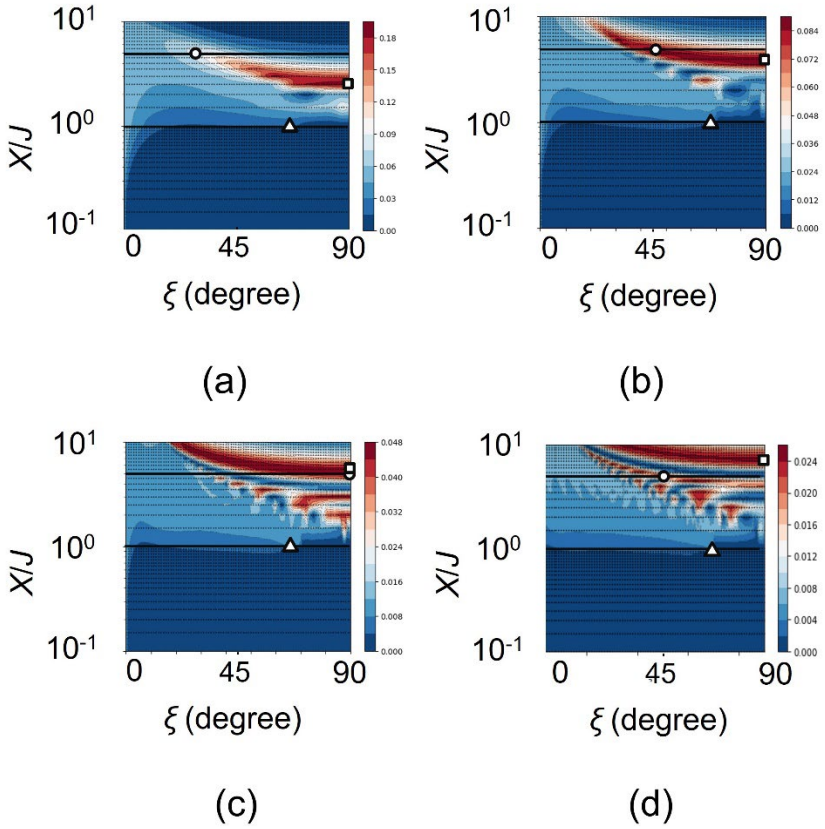

Fig.8 Dependence of P on ξ and χ/J in the case with DPP energy dissipation.
n is 5 (a), 11 (b), 21 (c), and 41 (d). △ and ○ on the horizontal line of χ/J=1 and 5, respectively, represent the position at which P takes the maximum P_{max}. □ is the position for P_{max} in the red belt.

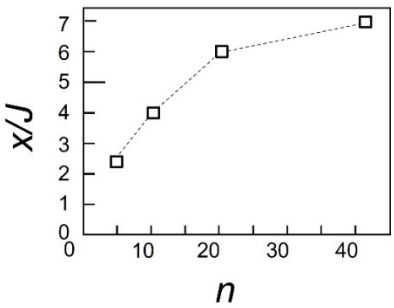

Fig. 9 Dependence of the value of χ / J at the position □ in Fig. 8 on n.

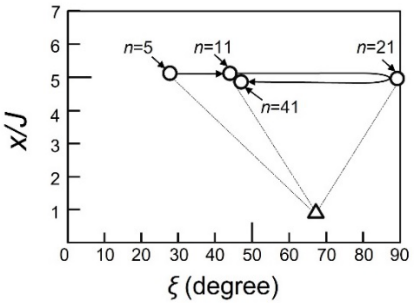

Fig.10 The value of ξ (at the position ○ in Fig. 8) at which P takes the maximum $P_{\max}$ at χ / J=5.

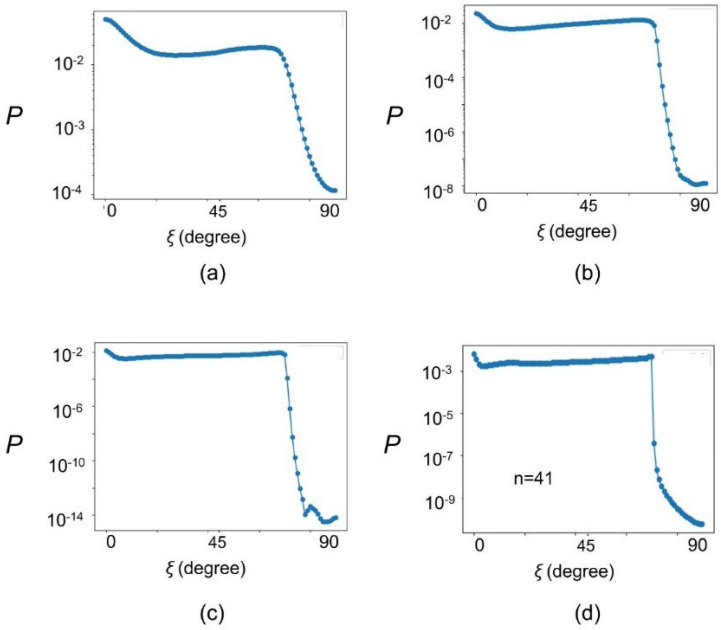

Fig. 11 Dependence of P on ξ at χ / J=1.
n is 5 (a), 11 (b), 21 (c), and 41 (d).

The value of P at the area isolated from the red belt is now evaluated for studying its regular and smooth variations. For this evaluation, χ / J is fixed to 1 (as was recommended in ref. [7]), and the dependence of P on ξ and n is derived as shown by Fig. 11. In contrast to Fig. 4, no bumps are seen on the curves in this figure, which indicates that no interference takes place in the triangular lattice. This is due to the absence of reflection at the slope and indicates that the present calculation results agree with the experimental results for the basic fiber probe in Fig. 2(b).

As in Case 1, the value of P in Fig. 11 takes the maximum $P_{\max}$ at ξ=67.5 degree (also at 0 degree), being independent of n. Figure 12 shows the dependence of the maximum $P_{\max}$ at ξ

=67.5 degree (and also at 0 degrees, for reference) on the value n. In contrast to Fig. 6, this figure shows that the maximum $P_{\max}$ decreases nearly monotonically with the increase of n. This is because the magnitude of the energy dissipation on the slope of the triangular lattice increases with the increase of n. However, the maximum $P_{\max}$ does not decrease drastically even though the value of n varies from 5 to 41. This indicates that a sufficiently high-energy DPP reaches the tip of the fiber probe even though the DPP energy dissipates from the slope. This is advantageous for practical applications.

Figure 13 shows the ratio between the maximum $P_{\max}$ and minimum $P_{\max}$ of each curve of Fig. 11. In contrast to Fig. 7, the ratio increases with the increase of n. Here, it should be noted that the values at n=21 deviates from the monotonically decreasing and increasing sequential lines in Figs. 12 and 13, respectively. In addition, the value of the ratio in Fig. 13 is much smaller than that in Fig. 7. Further discussions on Figs. 12 and 13 are required to compare them with Figs. 6 and 7.

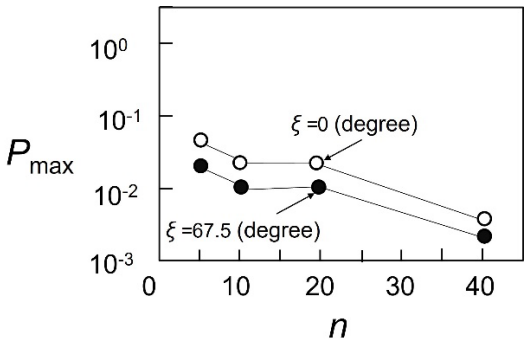

Fig. 12 Dependence of the maximum $P_{\max}$ (in Fig. 11) on n.

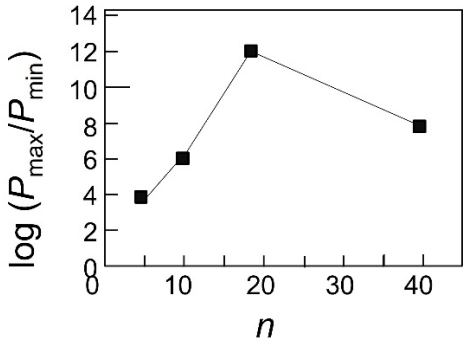

Fig. 13 Dependence of the ratio between the maximum $P_{\max}$ and minimum $P_{\min}$ (in Fig. 11) on n.

From the results and discussions for Case 1 and Case 2 above, the optimum value of the parameter ξ was found to be 67.5 degree, being independent of n. Furthermore, it was found that the value of the parameter χ / J can be fixed to 1, as was recommended in ref. [7]. It is expected that this value can be used even when the value of n is increased to $n > 41$ to increase the accuracy of approximating the fiber probe.

3.2. Temporal behaviors

Recent QW theoretical studies have found that the temporal behavior of the value of P exhibits pulsation prior to converging to the stationary value [9]. They have also found that the pulsation interval T_p is proportional to $\pi\sqrt{2N}$. Furthermore, the time T_s required to converge to the stationary value is proportional to $N \log N$. Here, $N\,(=n(n+1)/2)$ is the total number of sites in the triangle. Figure 14 shows an example of the temporal behavior of the value of P derived by the present calculations. The horizontal axis represents time. Figures 15 (a) and (b) show the values of T_p and T_s, respectively, calculated for **Case 2**. The horizontal axes represent the total number N of sites. The theoretical values above are represented by the curve A that monotonically increases with the increase of N. The curve B is the calculated result for χ/J=1. The curves C to E represent the calculated results for χ/J=5, in which the values of T_p and T_s increase with the increase of N, without exhibiting any irregular variations. This means that they do not suffer any effects from the red belt in Fig. 8, which is advantageous for comparing the results with the curve A.

By comparing the curves B to E with curve A, it can be concluded that the calculated temporal behaviors agree with the results derived by the QW theory, from which the validity of the present calculation is confirmed.

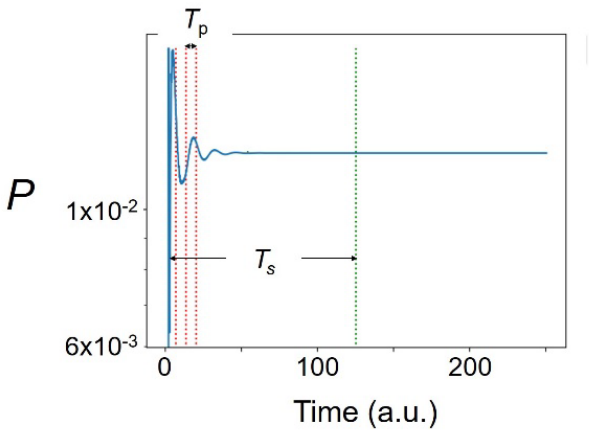

Fig. 14 An example of the calculated temporal behavior of the value of P.
The horizontal axis is proportional to time.

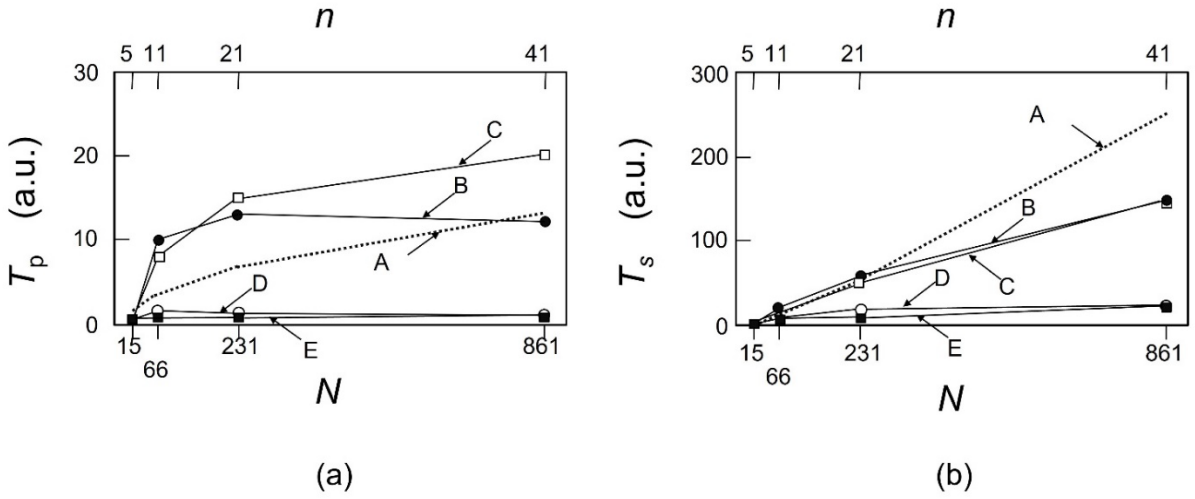

Fig. 15 Calculated values of the pulsation interval T_p (a) and the time T_s (b) required to converge to the stationary value.

The horizontal axis represents the total number N of sites in the triangular lattice. Curve A represents the theoretical values. Curve B represents the calculated values for χ / J =1. Curves C to E are the calculated values for χ / J =5 (at ξ =30, 60, and 90 degrees, respectively).

4. Summary

The present calculations successfully reproduced the DPP creation phenomena at the tip of a fiber probe. In particular, it was found that the value of the mathematical (ξ) and physical (χ / J) parameters could be fixed to 67.5 degree and 1, respectively, being independent of the parameter (n) for numerical calculation. It is expected that these values can be used to calculate the probability of the DPP creation at the tip of advanced high-throughput fiber probes, such as the asymmetric and triple-tapered fiber probes in Figs. 2(c) and (d), respectively. The calculated temporal behaviors agree with the results derived by the QW theory. It is expected that design criteria for novel fiber probes will be established in the near future based on the results of these calculations.

References

[1] M. Ohtsu, I. Ojima, and H. Sakuma, "Dressed Photon as an Off-Shell Quantum Field," *Progress in Optics* Vol.64, (ed. T.D. Visser) pp.45-97 (Elsevier, 2019).

[2] M. Ohtsu, *Off-Shell Applications In Nanophotonics*, Elsevier, Amsterdam (2021).

[3] H. Sakuma and I. Ojima, "On the Dressed Photon Constant and Its Implication for a Novel Perspective on Cosmology," *Symmetry* **2021**, 13, 593. https://doi.org/10.3390/sym13040593

[4] H. Sakuma, I. Ojima, M. Ohtsu and T. Kawazoe, "Drastic advancement in nanophotonics achieved by a new dressed

photon study, " *JEOS-RP* (2021)**17**:28.
https://jeos.springeropen.com/articles/10.1186/s41476-021-00171-w
[5] M. Ohtsu, *Dressed Photons*, Springer, Heidelberg (2014).
[6] M. Ohtsu, T. Kawazoe, and H. Saigo, "Spatial and Temporal Evolutions of Dressed Photon Energy Transfer," Offshell:1710R.001.v1.
DOI 10.14939/1710R.001.v1, http://offshell.rodrep.org/?p=79
[7] M. Ohtsu, "A Quantum Walk Model for Describing the Energy Transfer of a Dressed Photon," *Off-shell Archive* (September, 2021) OffShell: 2109R.001.v1.
DOI 10.14939/2109R.001.v1, http://offshell.rodrep.org/?p=345
[8] M. Ohtsu, Off-shell applications, Elsevier, 2021,p.9 (Fig.1.5)]
[9] M. Sabri, E. Segawa, "Sensitivity of quantum walk and dressed photon to perturbation," Abstracts of the 69nd Jpn. Soc. Appl. Phys. Spring Meeting, March 22-26, 2022, (Aoyama Gakuin Univ. and Online meeting), paper number 22a-E103-4.